

A Novel Method for Spatially-Selective ZnO Thin Film Growth by the Sol-Gel Technique

Arpita Das^{1,a}, Alakananda Das^{2,b}, Sayantani Sen^{3,c}, Anirban Bhattacharyya^{2,d}

¹ Institute of Engineering and Management, Kolkata, University of Engineering and Management, Kolkata 700160, India

² Institute of Radio Physics and Electronics, University of Calcutta, Kolkata 700009, India

³ Centre for Research in Nanoscience and Nanotechnology, University of Calcutta, Kolkata 70000106, India

^a arpita.das@uem.edu.in

^b adas4015@gmail.com

^c syantani163@gmail.com

^d anirban1@gmail.com

Abstract

Sol-gel deposition of ZnO using the dip-coating method typically generates uniform large area thin films on various substrates, and individual devices are created by a subsequent etching step. In this paper a method for the spontaneous formation of islands of ZnO aligned to existing electrode structures has been presented where thin films and nanostructures of ZnO were sequentially deposited on patterned substrates by sol-gel and vapor-liquid-solid processes. The results indicate spontaneous formation of spatially-selective structures of ZnO which avoid proximity to electrode edges. The morphology of these islands shows a honeycomb-like pattern with extended ridges, with ZnO nanowires depending on the underlying thin film, and are observed on the top of the ridge-like structures, thereby enhancing the surface area. This technique is well applicable for formation of ZnO-based sensor devices. Spatial selectivity of the deposition allows the development of semiconductor devices while eliminating the need of any chemical etching process step.

Keywords: ZnO thin film, Sol-gel, ZnO nanowire, VLS, Electrode geometry, Lift-off.

Received 27 January 2025; First Review 06 February 2025; Accepted 07 February 2025

* Address of correspondence

Dr. Anirban Bhattacharyya
Institute of Radio Physics and Electronics,
University of Calcutta, Kolkata 700009, India

Email: anirban1@gmail.com

How to cite this article

Arpita Das, Alakananda Das, Sayantani Sen, Anirban Bhattacharyya, A Novel Method for Spatially-selective ZnO Thin Film Growth by the Sol-Gel Technique, J. Cond. Matt. 2024; 02 (02): 37-42.

Available from:
<https://doi.org/10.61343/jcm.v2i02.69>



Introduction

In recent times, Zinc Oxide (ZnO) materials have been investigated tremendously, and form part of various electronic and optoelectronic devices currently in production [1-4]. Doped with Aluminum, ZnO are excellent transparent conducting oxide materials [5]. Since exciton binding energy in ZnO is very high, these materials are candidates for optical emitters that can operate at elevated temperatures. Unfortunately, the applications of these materials have been restricted so far due to inefficient p-type doping, in the recent years gradual progress have been made [6-7]. Several elements such as Al [8], Ga [9], Mg [10], Sn [11], as well as Mn [12] and Fe [13] have been used as a dopant in ZnO materials for controlling their electronic, optical and magnetic properties.

These materials have been grown by a number of processes, such as sol-gel [14], hydrothermal synthesis [15], vapor-liquid-solid (VLS) [16], sputtering [17], chemical vapor

deposition (CVD) [18] and gas-source molecular beam epitaxy (MBE) [19]. The use of the sol-gel technique is very widespread as this process lends itself to the deposition of large area, relatively uniform, high quality well-oriented polycrystalline thin films. The characteristics of the deposited thin film depends on the composition of the precursor solution, coating method applied, and annealing temperature employed [20]. This procedure is aimed to fabricate films of uniform nature, and the fabrication of devices are to be carried out using standard tools such as photolithography, metal deposition for electrode formation, and etching of the semiconducting thin film. It should be noted however that the fabrication of micro scale patterned metallic electrodes by chemical etching on top of ZnO thin films (doped or undoped) is quite challenging as the underlying film readily reacts with most acids at room temperature. Furthermore, the presence of grains and grain boundaries of the film makes it difficult to completely remove organic materials from the film surface after photoresist patterning if the lift-off process is employed.

In this work we discuss a novel deposition process where patterned electrodes are deposited on to the top surface of a sapphire substrate first and then the sol-gel technique is applied, and we demonstrate self-limiting, well-aligned formation of ZnO patterns that do not require any additional lithography or etching steps.

Method

Platinum electrodes in the configuration shown in figure 1(a) were patterned on to (0001) sapphire substrates [Monocrystal, Russia], using image reversal lift-off photolithography and sputter coating (Quorum Technology Q150V) processes.

Sol-gel dip-coating method was used for depositing thin films of ZnO on the substrate with electrodes already fabricated on it. The precursor element was Zinc acetate dihydrate ($\text{Zn}(\text{CH}_3\text{COO})_2 \cdot 2\text{H}_2\text{O}$), which was dissolved in Isopropanol (IPA) and finally a 0.5M solution was produced. Diethanolamine (DEA) ($\text{HN}(\text{CH}_2\text{CH}_2\text{OH})_2$) was incorporated as a stabilizer at 1:1 ratio within the solution. The precursor solution was kept on a magnetic hot plate and continuously stirred at 60 °C for 2 hours. Aluminum Nitrate Nonahydrate ($\text{Al}(\text{NO}_3)_3 \cdot 9\text{H}_2\text{O}$) was added to the solution for Al doping and finally 3% Al doped solution was prepared. The solution was stabilized for 24 hours before dip coating. The substrates with pre-fabricated platinum electrodes were dip-coated into the precursor solution and slowly raised at the rate of 1mm/s to complete the coating process, before being preheated at 150°C for 15 minutes. The whole procedure was repeated twice before the final anneal step at 500 °C in air for 60 minutes.

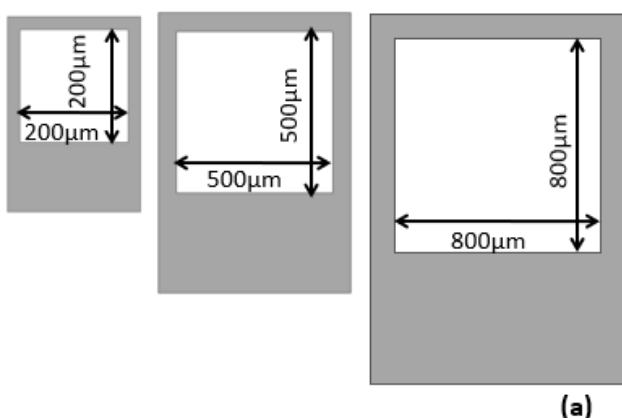


Figure 1(a): Electrode geometry with dimensions

Subsequently, ZnO nanostructures were grown using VLS process on the fabricated thin films. 1nm Gold (Au) thin films were sputter-coated, before annealing at 900°C–925°C for 30 minutes in presence of Argon to form Au nano droplets. Equal mixture of Zinc oxide and graphite powder were kept in a quartz boat at 950°C-975°C and the Au-coated substrates were placed downstream kept at 800°C-

825 °C. The entire reaction was performed for 30 minutes in Argon ambience, where flow rate is kept at 5sccm. The entire experimental procedure is described in figure 1(b).

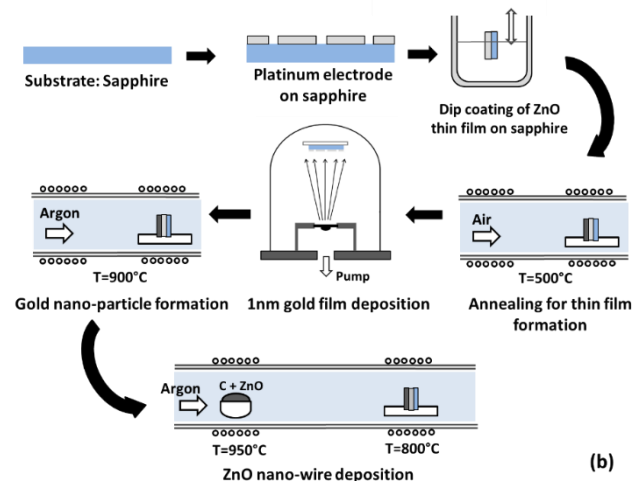


Figure 1(b): Experimental procedure

Results

Electrode geometry

The novelty of the current approach centers around the use of already-patterned substrates, that is the use of sapphire substrates with the electrodes already formed on them, before carrying out the deposition processes. It was found, as will be expanded in subsequent sections, that the configuration that is the shape and size of the electrodes play a very significant role in the final results obtained. This is presented in figure 1(a), where a three-electrode cluster is shown. This pattern has been repeated over the wafer. The electrodes are designed as ‘square rings’, that is the metal is bounded by an outer and an inner rectangle, set off center with respect to each other. The wider ‘pad’ part at the bottom was designed for probing or wire bonding, as needed. The dimensions are provided in figure 1(a), and the overall dimensions of the electrodes E1, E2 and E3 are 800µm x 800µm, 500µm x 500µm and 200µm x 200µm respectively. The width of the thinnest part was 100µm, 60µm and 40µm respectively. The separation between two adjacent electrodes was 200µm. It should be noted that the thickness of the platinum metal was 10nm.

Optical Microscopy

After the sol-gel growth of ZnO thin film [21], ZnO nanowires were deposited subsequently by the VLS process [16], and the samples were studied using optical microscopy at various magnifications. While there are small variations, the devices were found to exhibit nearly identical features. In figure 2, two representative images of the large electrode E1 is shown on the top row. The rectangular metallic electrode geometry is clearly visible for all the devices,

indicating that they have survived the high temperature processes that they were subjected to. The horizontal scratch marks exposing the metal across the bottom “pad” portion of the device was made by probes during electrical testing, and may be ignored for the current discussion.

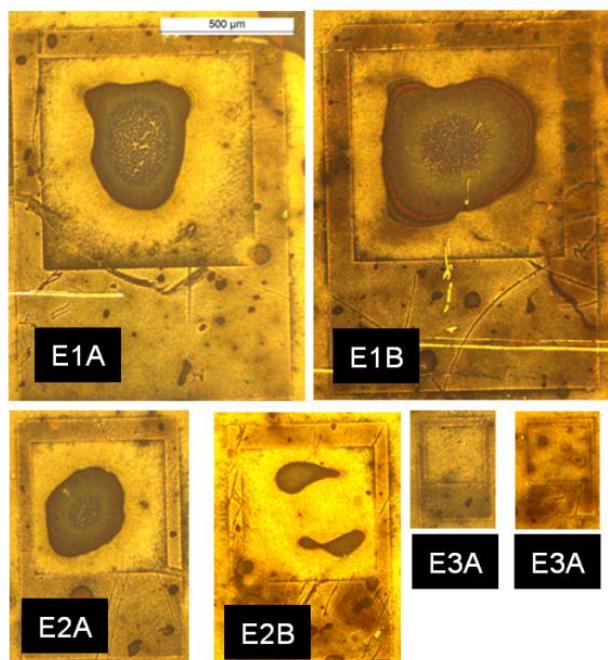


Figure 2: Optical microscope images of electrode E1 (largest electrode of device A and B), E2 (medium sized electrode of device A and B) and E3 (smallest sized electrode of device A and B)

The point of interest is that for both the devices E1A and E1B, and for all similar devices, the active region enclosed by the electrode was found to be nonuniform, with prominent irregular shaped islands being observed as dark patches. While the exact shape of the patch randomly varies, they are always clearly isolated from the inner edges of the electrode, occupy the central part, and cover 60-70% of the area. When the medium size devices were investigated, they show similar features as shown by E2A and E2B of the bottom row. However, there are clear difference that occur for these devices when compared to that for the larger ones. The central patch is present in all devices, but they are more irregular in shape, and may consist of two patches, well separated from each other, instead of a central single one. It is interesting to note that for most of the smallest devices, there are no central patch, and the devices show uniformity over the entire area. This is shown in figure 2, for the devices E3A and E3B, shown in the bottom row. It should be noted that even for these smaller devices, the electrode patterns are clear and do not show sign of any process-induced damage.

Energy Dispersive Spectroscopy (EDS) Measurements

EDS measurements were performed to investigate the chemical analysis of the samples, using an acceleration

voltage of 15KV for enhancing the SNR and reduce scan time. At this voltage, the electron beam is expected to penetrate the thin ZnO film into the sapphire Al_2O_3 substrate below. The overall EDS measurement indicates the existence of Zn, Al, O, and Pt elements. Figure 3(a) indicates the images obtained from scanning electron microscopy for a quarter of the device, showing the patch, as described previously, here appearing lighter over a darker background, and the platinum electrode, the edge of which has been highlighted by dashed lines. The spatial distribution of Al, which is present in the substrate below, is shown in figure 3(b), which as expected is uniform, with a darker region indicating the platinum electrode region, as the electrons are absorbed on the way down in the thin platinum film. The patch is observed to be dark for the same reason. When Zn is mapped over the device, it is clear that there are two distinct regions. A thinner layer of ZnO is present all over the surface, as indicated as the presence of uniform but sparse distribution of pink dots in figure 3(c). However, the patch shows a significantly higher presence of Zn, indicating the it is due to the presence of a much thicker film of ZnO, that has been selectively deposited at the central regions of each of the devices, in a spontaneous but extremely reliable manner. The importance of this finding is that spatial selectivity is very crucial to achieve for sol-gel process as well as VLS deposition.

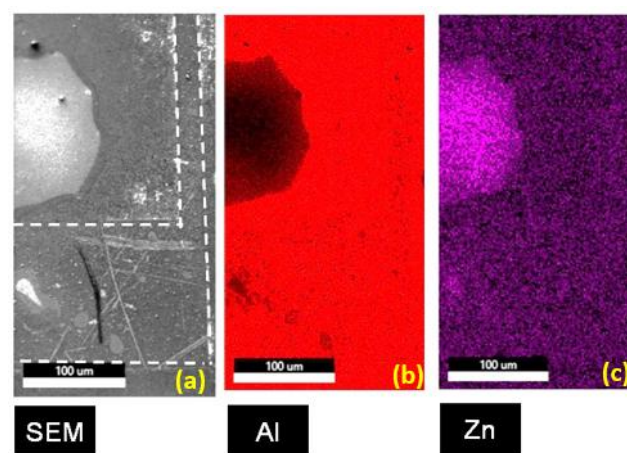


Figure 3: SEM Image (a) and EDS Image indicating the presence of Al (b) and Zn (c).

Scanning Electron Microscopy (SEM)

EDS mapping showed that the thickness of the ZnO thin film was significantly higher at the center of the device windows. Detailed scanning electron microscopy was performed to investigate this fact further, and the results were presented in figure 4. An SEM image of the electrode E1A, whose optical microscopy image was presented earlier, is shown in figure 4(a).

The metallic electrode pattern is again clearly visible. The dark patch at the center of the device is shown here as a grey area, which we name Z_1 (Zone 1). The region around this

patch is darker and very uniform, which we term Z_2 (Zone 2), while the region around the edge of the electrode appears significantly brighter, showing unresolved dots-like features at this magnification is Z_3 (Zone 3). High magnification images were obtained at each of these zones, which are presented in the figures 4(b) to 4(e). It would help to recall that the surface of the sample is expected to show features arising from the sol-gel process as well as the VLS process carried out subsequently.

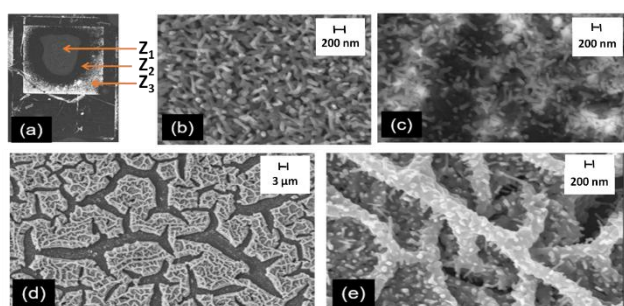


Figure 4: Low magnification SEM image of ZnO inside electrode E1 is shown in (a) along with high magnification SEM images of zones Z_2 (b), Z_3 (c) and Z_1 (d, e).

The surface morphology obtained from the Zone immediately around the patch area Z_2 indicates the presence of densely packed nanowires, with lengths of $200\mu\text{m}$ and diameters about $50\mu\text{m}$. Similar features are also present in the zone Z_3 but the nanowire density is lower. For both these regions, the features are similar to results obtained for ZnO nanostructures fabricated by the VLS process on to ZnO thin films deposited by sol-gel, as presented in our early publications [16]. However, the morphology is significantly different for zone Z_1 , that is spontaneously positioned at the center of each of the devices. Here, as observed by EDS, the film is significantly thicker. This can be easily correlated with the SEM image as shown in lower magnification in figure 4(d), which shows a thicker ZnO film with honeycomb-type morphology formed by branched ridges separated by deep trenches. The higher magnification image of this area, as seen in figure 4(e) indicates the presence of ZnO nanowires, which have been grown on top of the ridge-like features.

Discussion

The critical element that has been highlighted in the previous sections is that the existence of a thicker “patch” of ZnO film of roughly the same size, spontaneously deposited at the center of the device. A possible mechanism driving this spontaneous formation is shown schematically in figure 5. Figure 5(a) indicates the cross-section of a sapphire substrate, on to which platinum electrodes were specifically patterned as described in figure 5(b). During the sol-gel dip-coating process, the patterned substrate was dipped into the precursor solution and subsequently withdrawn slowly.

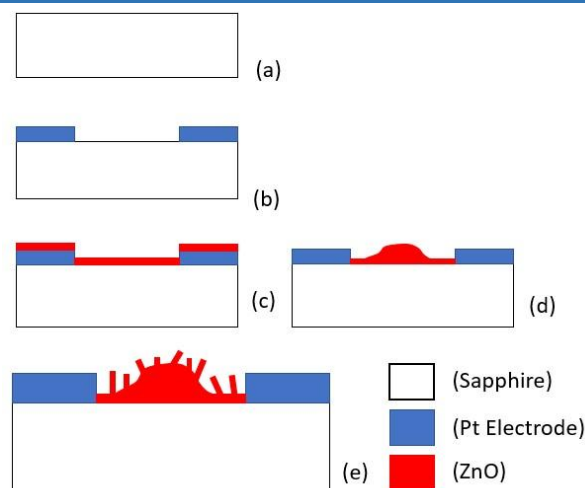


Figure 5: Schematic indicating mechanism for formation of ZnO spatially-selective structures (a) Substrate, (b) Electrode formation, (c) thin film deposition by sol-gel, (d)-(e) Nanowire by VLS.

This coats all areas, including the bare sapphire substrate as well as tops of platinum electrodes. After the withdrawal of the sample from the solution, it cannot be expected that precursor solution wets both these surfaces equally. A difference of hydrophobicity, and hence of the contact angles formed, is present at the precursor/sapphire and precursor/platinum interfaces. We believe that the liquid withdraws spontaneously from top of the platinum and is “pooled” at the center of the device, on the bare sapphire substrate, as depicted in figure 5(c). With the evaporation of the isopropyl alcohol, this forms a thicker patch of “gel” at the center of the device, which subsequently is annealed to form the ZnO film, onto which the VLS grown nanowires have been deposited (figure 5(d)-(e)). This model based on the flow of precursor solution away from the top of platinum electrodes can be justified based on the observation of smaller samples. For smaller platinum area, the formation of the ZnO thicker patch is less regular. Furthermore, this mechanism is completely absent for the smallest device. However, it should be stressed that further studies in contact angle measurement and real-time study of the sol-gel dip coating process are needed to establish and quantify the processes involved.

The generation of thicker films within the area demarcated by the electrodes is technologically very attractive, especially as such films contain a ridged morphology, having higher surface to volume ratio compared to other regions. Furthermore, the ratio was significantly enhanced by the deposition of VLS grown ZnO nanowires. This is of importance to a wide range of devices, including gas and liquid sensors, photodetectors, etc.

Conclusion and Future Prospective

While growth of ZnO by the sol-gel technique has been

extensively studied, this process is restricted to generation of thin films of uniform thickness. In this work we demonstrate a process for the spontaneous formation of ZnO islands, that are automatically placed at the center of ring-type electrodes. These islands show a ridged network type morphology, having very high surface to volume ratio. Furthermore, nanowires were grown on to these islands using VLS process, to further increase the surface area. This process is possibly driven by surface tension forces, based on difference in wettability of the electrode or substrate surface for the precursor solution. These findings are expected to find major applications in development of sensor devices.

Acknowledgement

Alakananda Das (09/028 (0946)/2015-EMR-I) and Sayantani Sen (09/028(0921)/2014-EMR-I) would like to acknowledge the CSIR Senior Research Fellowship scheme. The authors would like to acknowledge University of Calcutta for SEM and EDS measurement.

References

1. A. Janotti, C. G. Vande Walle, "Fundamentals of zinc oxide as a semiconductor", Rep. Prog. Phys.72, (2009), 126501. <https://doi.org/10.1088/0034-4885/72/12/126501>
2. A. K. Radzimska, T. Jesionowski, "Zinc Oxide—From Synthesis to Application: A Review", Materials 7, (2014),2833–2881. <https://doi.org/10.3390/ma7042833>
3. U. Ozgur, D. Hofstetter, H. Morkoc, "ZnO Devices and Applications: A Review of Current Status and Future Prospects", Proc. IEEE 98(7), (2010), 1255–1268. <https://doi.org/10.1109/JPROC.2010.2044550>
4. B. K. Sonawane, M. P. Bhole, D. S. Patil, "Structural, optical and electrical properties of post annealed Mg doped ZnO films for optoelectronics applications", Opt. Quant. Electron 41, (2009), 17–26. <https://doi.org/10.1007/s11082-009-9317-y>
5. M. C. Jun, J. H. Koh, "Optical and structural properties of Al-doped ZnO thin films by sol gel process", J Nanosci Nanotechnol. 13(5), (2013), 3403-7. <https://doi.org/10.1166/jnn.2013.7314>
6. C. H. Park, S. B. Zhang, Su-Huai Wei, "Origin of p-type doping difficulty in ZnO: The impurity perspective", Phys. Rev. B 66, (2002), 073202. <https://doi.org/10.1103/PhysRevB.66.073202>
7. Z. Ye, H. He, L. Jiang, "Co-doping: an effective strategy for achieving stable p-type ZnO thin films", Nano Energy 52, (2018), 527-540. <https://doi.org/10.1016/j.nanoen.2018.08.001>
8. Y. S. Kim, W. P. Tai, "Electrical and optical properties of Al-doped ZnO thin films by sol-gel process", Appl. Surf. Sci. 53(11), (2007), 4911-4916. <https://doi.org/10.1016/j.apsusc.2006.10.068>
9. V. Bhosle, A. Tiwari, J. Narayan "Electrical properties of transparent and conducting Ga doped ZnO", J. Appl. Phys. 100, (2006), 033713. <https://doi.org/10.1063/1.2218466>
10. K. Huang, Z. Tang, L. Zhang, J. Yu, J. Lv, X. Liu, F. Liu, "Preparation and characterization of Mg-doped ZnO thin films by sol-gel method", Appl. Surf. Sci. 258(8), (2012), 3710-3713. <https://doi.org/10.1016/j.apsusc.2011.12.011>
11. M. Ajili, M. Castagné, N. K. Turki, "Study on the doping effect of Sn-doped ZnO thin films", Superlattices Microstruct. 53, (2013), 213-222. <https://doi.org/10.1016/j.spmi.2012.10.012>
12. S. A. Ahmed, "Structural, optical, and magnetic properties of Mn-doped ZnO samples", Results in Physics 7, (2017), 604-610. <https://doi.org/10.1016/j.rinp.2017.01.018>
13. A. K. Mishra, D. Das, "Investigation on Fe-doped ZnO nanostructures prepared by a chemical route", Materials Science and Engineering: B171, (2010), 1–3. <https://doi.org/10.1016/j.mseb.2010.03.045>
14. K. Davis, R. Yarbrough, M. Froeschle, J. White, H. Rathnayake, "Band gap engineered zinc oxide nanostructures via a sol-gel synthesis of solvent driven shape-controlled crystal growth", RSC Adv.9, (2019), 14638-14648. <https://doi.org/10.1039/C9RA02091H>
15. S. Baruah, J. Dutta, "Hydrothermal growth of ZnO nanostructures", Sci. Technol. Adv. Mater. 10, (2009), 013001. <https://doi.org/10.1088/1468-996/10/1/013001>
16. P. G. Roy, A. Dutta, A. Das, S. Sen, P. Pramanik, A. Bhattacharyya, "VLS-grown diffusion doped ZnO nanowires and their luminescence properties", Mater. Res. Express 2 (2015) 075007. <https://doi.org/10.1088/2053-1591/2/7/075007>
17. M. Maslyk, M.A. Borysiewicz, M. Wzorek, T. Wojciechowski, M. Kwoka, E. Kamińska, "Influence of absolute argon and oxygen flow values at a constant ratio on the growth of Zn/ZnO nanostructures obtained by DC reactive magnetron sputtering", Appl. Surf. Sci. 389, (2016), 287-293. <https://doi.org/10.1016/j.apsusc.2016.07.098>
18. L. N. Protasova, E. V. Rebrov, K. L. Choy, S. Y. Pung, V. Engels, M. Cabaj, A. E. H. Wheatley, J. C. Schouten, "ZnO based nanowires grown by chemical vapour deposition for selective hydrogenation of acetylene alcohols", Catal. Sci. Technol.1, (2011), 768-777. <https://doi.org/10.1039/C1CY00074H>

-
19. J. S. Wang, C. S. Yang, P. I. Chen et al., “Catalyst-free highly vertically aligned ZnO nanoneedle arrays grown by plasma-assisted molecular beam epitaxy,” *Applied Physics A*, 97(3), (2009), 553–557.
<https://doi.org/10.1007/s00339-009-5436-3>
 20. L. Znaidi, “Sol-gel-deposited ZnO thin films: A review”, *Materials Science and Engineering: B*, 174(1–3), (2010).
<https://doi.org/10.1016/j.mseb.2010.07.001>
 21. A. Das, P. G. Roy, A. Dutta, S. Sen, P. Pramanik, D. Das, A. Banerjee, A. Bhattacharyya, “Mg and Al co-doping of ZnO thin films: Effect on ultraviolet photoconductivity”, *Materials Science in Semiconductor Processing*, 54, (2016), 36-41.
<https://doi.org/10.1016/j.mssp.2016.06.018>